
FocusFormer: Focusing on What We Need via Architecture Sampler

Jing Liu Jianfei Cai Bohan Zhuang[†]

Department of Data Science & AI, Monash University, Australia

Abstract

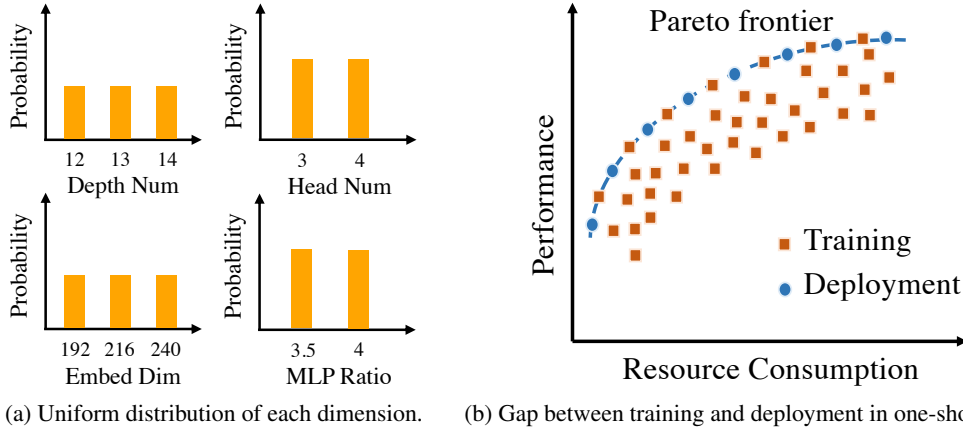
Vision Transformers (ViTs) have underpinned the recent breakthroughs in computer vision. However, designing the architectures of ViTs is laborious and heavily relies on expert knowledge. To automate the design process and incorporate deployment flexibility, one-shot neural architecture search decouples the supernet training and architecture specialization for diverse deployment scenarios. To cope with an enormous number of sub-networks in the supernet, existing methods treat all architectures equally important and randomly sample some of them in each update step during training. During architecture search, these methods focus on finding architectures on the Pareto frontier of performance and resource consumption, which forms a gap between training and deployment. In this paper, we devise a simple yet effective method, called FocusFormer, to bridge such a gap. To this end, we propose to learn an architecture sampler to assign higher sampling probabilities to those architectures on the Pareto frontier under different resource constraints during supernet training, making them sufficiently optimized and hence improving their performance. During specialization, we can directly use the well-trained architecture sampler to obtain accurate architectures satisfying the given resource constraint, which significantly improves the search efficiency. Extensive experiments on CIFAR-100 and ImageNet show that our FocusFormer is able to improve the performance of the searched architectures while significantly reducing the search cost. For example, on ImageNet, our FocusFormer-Ti with 1.4G FLOPs outperforms AutoFormer-Ti by 0.5% in terms of the Top-1 accuracy.

1 Introduction

With powerful computing resources and large amounts of labeled data, we have witnessed the tremendous successful applications of ViTs in computer vision [54, 14, 37]. To push the state-of-the-art performance boundary, several studies [58, 37, 10, 55] have been proposed to craft the architectures of ViTs and achieved competitive performance in many visual tasks, such as image classification [14, 54, 69] and dense prediction [6, 73, 9]. However, manually designing ViT architectures is laborious and human expertise is often sub-optimal in exploring the huge design space.

To automatically design ViT architectures, much effort has been devoted to neural architecture search (NAS) [43, 36, 5, 50] by finding optimal architectures in a predefined search space. To obtain compact architectures, some works [36, 60, 72] propose to search architectures for a specific resource constraint or hardware requirement. Nevertheless, when it comes to diverse platforms under various resource constraints (*e.g.*, FLOPs, latency, on-chip memory), these methods need to design architecture for each scenario from scratch and the search cost grows linearly with the number of possible cases, which is extremely computationally expensive. To tackle the above issue, one-shot NAS methods [23, 16, 65, 18, 7] have been proposed to decouple the model training and the

[†]Corresponding author. Email: bohan.zhuang@monash.edu



(a) Uniform distribution of each dimension. (b) Gap between training and deployment in one-shot NAS.

Figure 1: An overview of the uniform distribution of each architectural dimension and the gap between training and deployment in one-shot NAS methods [65, 7]. During supernet training, existing methods randomly sample sub-networks (rectangle) from a uniform architectural distribution in one update step. During deployment, these methods focus on the sub-networks (circle) on the Pareto frontier of performance and resource consumption. The other architectures that are not on the Pareto frontier are neglected.

architecture search stage, where the first stage trains an over-parameterized supernet that covers a considerable number of sub-networks (*e.g.*, 10^{20}) with diverse architectural configurations and the second stage selects an optimal sub-network given the target resource constraint during deployment.

Nevertheless, there exists a gap between training and deployment. Specifically, to deal with the tremendous number of sub-networks in supernet, existing methods [23, 4, 57, 65] randomly sample some of them from a uniform architectural distribution (See Figure 1a) in each update step during training, where all architectures in the search space (rectangles in Figure 1b) have an equal probability of being chosen. During deployment, these methods focus on those architectures (circles in Figure 1b) that are on the Pareto frontier of performance and resource consumption. The other architectures (rectangles not on the Pareto frontier) that have poor performance or do not meet the resource constraint are neglected. In this case, the training stage does not concentrate on the architectures on the Pareto frontier. As a result, the architectures with good performance may not be sufficiently trained and hence the performance of the searched architectures is sub-optimal. Moreover, after supernet training, existing methods have to either use evolutionary search [23, 4, 65, 7] or train a controller [64, 48] to search for optimal architectures given a deployment scenario, which requires extensive architecture evaluations and hence incurs high computational cost.

In this paper, we devise a simple yet effective method, called *FocusFormer*, to bridge the gap between training and deployment. Unlike existing NAS methods for ViTs [65, 7], we assume and highlight that not all sub-networks in the supernet are equally important. Based on this intuition, we devise a parameterized architecture sampler to learn the architectural distribution under diverse resource constraints, where we consider four important dimensions of ViTs including depth, embedding dimension, multi-layer perceptron (MLP) ratio, and head number. Instead of sampling from a uniform architectural distribution, we optimize the architecture sampler to generate sampling distributions conditioned on different resource constraints to assign higher probabilities to accurate sub-networks in an update step. In this way, we are able to train sub-networks that are likely to be on the Pareto frontier with more training budgets, thereby improving their performance. Once the supernet and architecture sampler have been well-trained, we can directly use the architecture sampler to instantly generate candidate ViT architectures with good performance given the target resource constraint in the architecture search stage. Therefore, our *FocusFormer* does not need to involve extensive architecture evaluations such as in evolutionary methods [65, 46] and hence greatly improve the search efficiency. Extensive experiments on CIFAR-100 and ImageNet show that our proposed method improves the performance of the searched architectures while significantly reducing the search cost.

Our main contributions are summarized as follows:

- We propose *FocusFormer* to bridge the gap between training and deployment in one-shot NAS for ViTs. To our knowledge, this problem has not been well studied.

- We design a parameterized architecture sampler to serve as the bridge. During supernet training, the architecture sampler is jointly optimized with network parameters to identify and assign higher sampling probabilities for architectures on the Pareto frontier under different resource constraints, that align with the searched networks at the specialization stage. In this way, we allocate more training resources to these salient architectures and thus improve their performance. During deployment, we can instantly find the target candidate architectures for a given resource constraint using the well-trained architecture sampler, with very high search efficiency.
- We evaluate our proposed method on CIFAR-100 and ImageNet. Extensive experiments demonstrate that our proposed method is able to improve the performance of the specialized network while greatly reducing the search cost. For example, on ImageNet, our FocusFormer-Ti surpasses AutoFormer-Ti by 0.5% on the Top-1 accuracy.

2 Related Work

Vision Transformers. Recently, ViTs [14, 6, 37, 73] have shown great representational power in computer vision. Specifically, a ViT [14] contains a patch embedding layer, multiple Transformer blocks, and a task-dependent head, where each Transformer block consists of a multi-head self-attention (MSA) block and an MLP block. LayerNorm (LN) [1] and residual connection [27] are applied before and after each block, respectively. To improve the performance of ViTs, several methods are proposed, including but not limited to incorporating hierarchical representations [17, 42, 37, 58], introducing inductive bias by inserting convolutional layers [61, 35, 66, 20, 15, 8, 19, 26] and improving positional encoding [11, 62], *etc.* Though achieving promising performance, the ViT architectures of these methods are manually designed, which may not fully explore the architecture space. Compared with these methods, our proposed FocusFormer focuses on automatically designing the ViT architecture.

Neural architecture search. Neural architecture search (NAS) [75, 43, 36] seeks to automatically find architectures with promising performance while satisfying the resource constraint B , which can be formulated as

$$\begin{aligned} & \min_{\alpha} \mathcal{L}_{\text{val}}(W_{\alpha}^*; \mathcal{D}_{\text{val}}) \\ \text{s.t. } & W_{\alpha}^* = \arg \min_{W_{\alpha}} \mathcal{L}_{\text{train}}(W_{\alpha}; \mathcal{D}_{\text{train}}), C(\alpha) < B, \end{aligned} \quad (1)$$

where W_{α} is the weights of the network with architecture α , $C(\alpha)$ is the computational cost of α , and $\mathcal{L}_{\text{train}}$, \mathcal{L}_{val} are the training loss and validation loss, respectively. Here, $\mathcal{D}_{\text{train}}$ and \mathcal{D}_{val} are the training and validation dataset, respectively. To solve Problem (1), we have to train weights W_{α} for each architecture α until convergence to obtain W_{α}^* , which takes unbearable computational cost. Most existing approaches either use random search [34, 2], reinforcement learning [75, 22, 43, 52], evolutionary search [41, 40, 46, 47] or gradient-based optimization [36, 5, 60, 25] to find optimal architectures.

In addition, one-shot NAS [4, 23, 16, 65, 7, 18] has been proposed to decouple the model training stage and architecture search stage. In the model training stage, the goal is to train an over-parameterized supernet that supports many sub-networks of different configurations with the shared parameters to accommodate different deployment scenarios. Let W be the weights of the supernet. The objective function for the supernet training can be formulated as

$$W^* = \arg \min_W \mathbb{E}_{\alpha \in \mathcal{A}} [\mathcal{L}_{\text{train}}(S(W, \alpha))], \quad (2)$$

where $S(W, \alpha)$ is a selection function that chooses a part of parameters from W to constitute the sub-network with architecture configuration α and \mathcal{A} is the architecture search space. To solve Problem (2), existing methods [65, 7] assume that all the sub-networks are equally important and use a uniform sampling strategy to approximate the expectation term. Considering different resource constraints, Problem (2) can be rewritten as

$$W^* = \arg \min_W \mathbb{E}_{B \sim \mathcal{B}} [\mathbb{E}_{\alpha \sim U(\cdot|B)} [\mathcal{L}_{\text{train}}(S(W, \alpha))]], \quad (3)$$

where B is a resource constraint sampled from a prior distribution \mathcal{B} and $U(\cdot|B)$ is a uniform distribution over architectures conditioned on B . For the architecture search stage, the goal is to obtain the specialized sub-network that satisfies the resource constraint B given a deployment

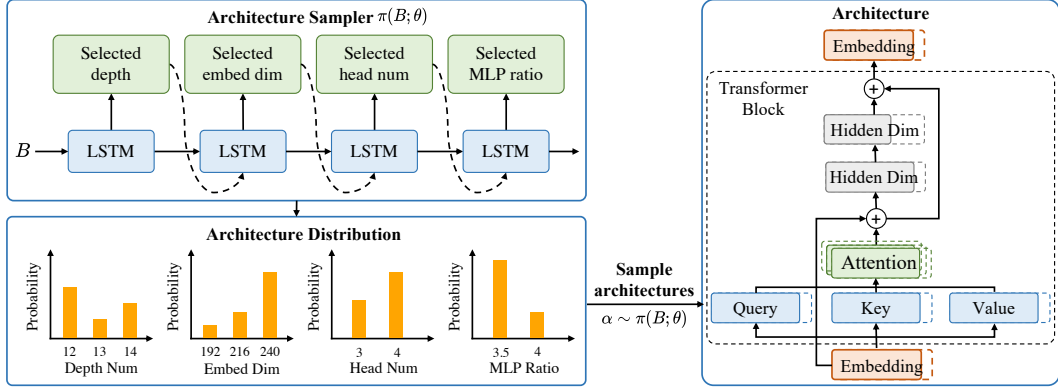


Figure 2: An illustration of our proposed architecture sampler. We formulate the architecture search problem as a sequential prediction problem where each element of the sequence denotes an architectural dimension of a ViT. Starting from a prior resource distribution \mathcal{B} , we first sample a resource constraint $B \sim \mathcal{B}$. We then feed B into an LSTM network with four fully connected layers and output the architectural distribution $\pi(B; \theta)$. Last, we obtain the candidate architecture by performing sampling from the architectural distribution $\alpha \sim \pi(B; \theta)$.

scenario while maximizing the validation accuracy $\text{Acc}_{\text{val}}(S(W^*, \alpha))$, which can be formulated as

$$\begin{aligned} \max_{\alpha} \text{Acc}_{\text{val}}(S(W^*, \alpha)) \\ \text{s.t. } C(\alpha) < B. \end{aligned} \quad (4)$$

Here, W^* is the well-learned weight of the supernet in the model training stage. Except for the validation accuracy, one can also use the negative validation loss to measure the performance of the searched architectures [36, 5]. To solve Problem (4), existing methods either use evolutionary search [23, 4, 68, 57, 65, 7] or train a controller to search for optimal architectures [64, 48, 30]. Since the supernet has been well-trained, we are able to obtain any sub-network without any fine-tuning or retraining during the architecture search, which yields a much lower search cost compared with Problem (1). Compared with AutoFormer [65] and S3 [7], our proposed FocusFormer bridges the gap between training and deployment, which greatly improves the performance of the specialized sub-networks and search efficiency. Compared with GreedyNAS [67, 31] and AttentiveNAS [56], our FocusFormer differs in several aspects. First, our method focuses on searching ViT architectures while GreedyNAS and AttentiveNAS concentrate on searching the architectures of convolutional neural networks (CNNs). Second, they need to sample and rank multiple architectures for each iteration during supernet training, which introduces extensive computational overhead. In contrast, our FocusFormer trains an architecture sampler to obtain sub-networks in an efficient way. Third, they need to use evolutionary search to find architectures, which is computationally expensive. Our FocusFormer uses the well-trained architecture sampler to instantly generate ViT candidate architectures, which is extremely efficient.

3 FocusFormer

In one-shot NAS, the objectives for the model training stage in Eq. (3) and the architecture search stage in Eq. (4) are different, resulting in a gap between training and deployment. Specifically, existing methods [4, 68] assume that all sub-networks are equally important and perform a uniform sampling strategy during supernet training. However, during deployment, we only care about architectures on the Pareto frontier of performance under various resource constraints. In this case, the model training stage does not tailor for those specialized architectures on the best Pareto front. As a result, the architectures with good performance may not be sufficiently trained and hence lead to the sub-optimal performance. Moreover, once the supernet has been well-trained, we have to use either evolutionary search [23, 4] or train a controller [64, 48] to search for optimal architectures due to the different objectives between the model training and architecture search stages, which introduces additional training cost.

In this paper, we jointly learn an architecture sampler with network parameters to assign higher probabilities to architectures that are likely on the Pareto frontier under different resource constraints

Algorithm 1 Training algorithm for FocusFormer.

Input: Supernet \mathcal{N} with parameter W , architecture sampler $\pi(\cdot; \theta)$ with parameter θ , the number of training epoch T , training dataset $\mathcal{D}_{\text{train}}$, architecture sampler update interval τ , resource constraint distribution \mathcal{B} , learning rate η , hyper-parameter β .

- 1: Randomly initialize the supernet parameter W and architecture sampler parameter θ .
- 2: **for** $t \in \{1, 2, \dots, T\}$ **do**
- 3: **if** $t = n\tau, n \in \mathbb{N}^+$ **then**
- 4: Train architecture sampler $\pi(B; \theta)$ on $\mathcal{D}_{\text{train}}$.
- 5: **end if**
- 6: **for** each batch of data in $\mathcal{D}_{\text{train}}$ **do**
- 7: Sample a resource constraint $B \sim \mathcal{B}$.
- 8: Sample an architecture $\alpha \sim \pi(B; \theta)$.
- 9: Train supernet \mathcal{N} with α .
- 10: **end for**
- 11: **end for**

during supernet training. In this way, we put more training resources on these important ViT architectures and hence mitigate the gap between training and deployment. Once the supernet and architecture sampler have been well-trained, we can directly use our architecture sampler to select good candidate architectures given a specific resource constraint, which is extremely efficient.

3.1 Training Supernet with Architecture Sampler

Given a ViT supernet \mathcal{N} with parameter W , we design an architecture sampler $\pi(\cdot; \theta)$ parameterized by θ to obtain architectures with potentially good performance given arbitrary B . With the architecture sampler, we formulate the objective for the supernet training as

$$W^* = \arg \min_W \mathbb{E}_{B \sim \mathcal{B}} [\mathbb{E}_{\alpha \sim \pi(B; \theta)} [\mathcal{L}_{\text{train}}(S(W, \alpha))]]. \quad (5)$$

Here, if we replace $\pi(B; \theta)$ with the uniform distribution over architectures $U(\cdot|B)$ conditioned on B , Problem (5) is reduced to the original one-shot NAS problem in Eq. (3). Equipped with $\pi(\cdot; \theta)$, those ViT architectures that are potentially on the Pareto frontier are trained with more computing resources. In this way, the gap between training and deployment can be mitigated and hence improve the performance of the searched architectures under different resource constraints. We summarize our training pipeline in Algorithm 1. Note that training the architecture sampler for each epoch is computationally expensive and not necessary. To reduce the computational cost, we only update our architecture sampler per τ epoch.

3.2 Learning Architecture Sampler

To determine the ViT architecture, we formulate the NAS problem as a sequence prediction problem where each element of a sequence denotes an architectural dimension (*e.g.*, the depth of ViT) following [43, 75]. To predict the architectural distribution, our architecture sampler $\pi(\cdot; \theta)$ is an LSTM network with four fully connected layers, which takes a resource constraint B as input and then outputs four architectural dimensions of a ViT, including depth, embedding dimension, head number and MLP ratio, as shown in Figure 2. We then perform sampling from the architectural distribution to obtain architectures, *i.e.*, $\alpha \sim \pi(B; \theta)$. To represent different B , we build learnable embedding vector for each B following [43, 21].

To train $\pi(\cdot; \theta)$, we formulate the objective function as

$$\max_{\theta} \mathbb{E}_{B \sim \mathcal{B}} [\mathbb{E}_{\alpha \sim \pi(B; \theta)} [R(W, \alpha)]], \quad (6)$$

where $R(W, \alpha)$ is a performance metric of the sampled architecture α . To guide the training of $\pi(\cdot; \theta)$, we hope the resource consumption of α not only close to the given resource constraint B , but also achieves high accuracy following [3]. Considering both the resource constraint and accuracy, we have

$$R(W, \alpha) = \text{Acc}_{\text{val}}(S(W, \alpha)) - \beta \left| \frac{B}{C(\alpha)} - 1 \right|, \quad (7)$$

Algorithm 2 Training algorithm for architecture sampler.

Input: Supernet \mathcal{N} , architecture sampler $\pi(\cdot; \theta)$ with parameter θ , total training iterations K , training dataset $\mathcal{D}_{\text{train}}$, distribution of resource constraint \mathcal{B} , learning rate η , hyper-parameter β .

- 1: **for** $k \in \{1, 2, \dots, K\}$ **do**
- 2: Sample a batch of data from $\mathcal{D}_{\text{train}}$.
- 3: Sample a resource constraint $B \sim \mathcal{B}$.
- 4: Sample an architecture $\alpha \sim \pi(B; \theta)$.
- 5: Compute the reward $R(W, \alpha)$ using Eq. (7).
- 6: Update θ using Eq. (8).
- 7: **end for**

where $\text{Acc}_{\text{val}}(S(W, \alpha))$ is the validation accuracy of α with corresponding weights $S(W, \alpha)$ and β is a hyper-parameter that makes a balance between accuracy and resource consumption. In order to reduce the training cost of $\pi(B; \theta)$, we only compute the validation accuracy on a mini-batch of data rather than the whole validation data set. In general, Eq. (7) is not differentiable w.r.t. θ . Following [75, 43], we use reinforcement learning with policy gradient [59] to solve Problem (6). Specifically, we update θ by ascending the policy gradient, which can be formulated as:

$$\theta \leftarrow \theta + \eta R(W, \alpha) \nabla_{\theta} \log \pi(B; \theta), \quad (8)$$

where η is the learning rate of $\pi(\cdot; \theta)$. We summarized the training details of our proposed architecture sampler in Algorithm 2.

Note that our architecture sampler introduces some additional costs during supernet training. To reduce the training cost, we train the supernet using a progressive learning strategy following [53, 33]. Specifically, we gradually increase the image size from a small $S_0 \times S_0$ to the final $S_e \times S_e$ with a fixed patch size p . As a result, the number of patches is increased from S_0^2/p^2 to S_e^2/p^2 . However, in ViT, the size of positional encodings is related to the number of patches. To overcome this limitation, we proposed to use conditional positional encodings following [11].

Resource constraint distribution. In Eqs. (5) and (6), we introduce a prior distribution \mathcal{B} . For simplicity, we assume that \mathcal{B} is a uniform distribution, which indicates that all resource constraints have an equal probability of being sampled. Note that there are a large number of B in \mathcal{B} and we can not enumerate them all during training. To overcome this limitation, we perform quantization to obtain discrete resource constraint as $B = \text{round}(B/s) * s$, where $\text{round}(x)$ returns the nearest integer of a given value x and s is a step size of the round function. To represent a resource constraint with an arbitrary value, we use the linear interpolation method following [21, 44].

3.3 Efficient Architecture Search

Once we have well trained the supernet and the proposed architecture sampler, we now focus on obtaining architectures that satisfy the given resource constraint while achieving promising performance. Using the well-learned $\pi(\cdot; \theta)$, we are able to directly obtain good candidate architectures. Specifically, given a resource constraint B , we first sample multiple architectures from the predicted architectural distribution $\pi(B; \theta)$. We will repeat the sampling process if the sampled ViT architecture does not satisfy the resource constraint, *i.e.*, $C(\alpha) > B$. Last, we select the ViT architecture with the highest validation accuracy as the searched architecture. Since only a limited number of architecture evaluations are involved, the search cost of our method is much smaller than the existing one-shot NAS methods [33, 7].

4 Experiments

Datasets. We evaluate the proposed method on two image classification datasets, namely, CIFAR-100 [32] and ImageNet [13]. CIFAR-100 contains 100 classes, where each class has 500 training images and 100 testing images. ImageNet is a large-scale dataset that contains 1.28M training images and 50k validation images with 1k classes. To construct the validation set, we randomly sample 10k and 100k training samples from CIFAR-10 and ImageNet following [36, 65].

Search space. Following [65], we apply our proposed method to ViT search space with three different settings, namely, supernet-tiny, supernet-small and supernet-base. Each search space contains four

Table 1: Performance comparisons of different methods on ImageNet. * denotes that we obtain the results from [54]. ** indicates that we change the model to use conditional positional encodings [11] for fair comparisons.

Models	Top-1 Acc. (%)	Top-5 Acc. (%)	#Params (M)	FLOPs (G)	Resolution
ResNet-18 [27]	69.8	-	11.7	1.8	224
DeiT-Ti [54]	72.2	91.1	5.7	1.2	224
AutoFormer-Ti** [65]	74.6	92.3	5.7	1.3	224
FocusFormer-Ti (Ours)	75.1	92.8	6.2	1.4	224
ResNet-50 [27]	76.1	-	25.6	4.1	224
RegNetY-4GF* [45]	80.0	-	21.4	4.0	224
BoTNet-S1-59 [51]	81.7	95.8	33.5	7.3	224
T2T-ViT-14 [69]	81.7	-	21.5	6.1	224
DeiT-S [54]	79.9	95.0	22.1	4.7	224
ViT-S/16 [14]	78.8	-	22.1	4.7	384
TNT-S [24]	81.5	95.7	23.8	5.2	224
AutoFormer-S** [65]	81.4	95.6	24.3	5.1	224
FocusFormer-S (Ours)	81.6	95.6	23.7	5.0	224
ResNet152 [27]	78.3	-	60.2	11.6	224
ResNeXt101-64x4d [63]	79.6	-	83.5	15.6	224
ViT-B/16 [14]	79.7	-	86.6	17.6	384
DeiT-B [54]	81.8	95.6	86.6	17.6	224
AutoFormer-B** [65]	81.7	95.5	52.8	11.0	224
FocusFormer-B (Ours)	81.9	95.6	52.7	11.0	224

main dimensions to build transformer blocks: embedding dimension, the number of heads, MLP ratio and network depth. The detailed settings of each search space can be found in AutoFormer [65]. For convenience, we use “FocusFormer-Ti”, “FocusFormer-S” and “FocusFormer-B” to represent the architectures obtained by FocusFormer in the tiny, small and base search space, respectively.

Evaluation metrics. We measure the performance of different methods using the Top-1 and Top-5 accuracy. Following [49, 29], we use the floating-point operations (FLOPs) and the number of parameters (#Params) to measure the resource consumption and model size, respectively. Following [36], we also measure the training and search costs using the training and search durations on a single NVIDIA GeForce RTX 3090 GPU, respectively.

Implementation details. We train our model using a server with 8 V100 GPUs. Following [65], we train the supernet with the weight entanglement strategy. The supernet is trained for 500 epochs with a mini-batch size of 128 and 1024 on CIFAR-100 and ImageNet, respectively. We scale the learning rate according to the batch size with formula: $lr_{scaled} = \frac{5 \times 10^{-4}}{512} \times batchsize$ and use cosine rule [38] to decrease the learning rate. We use AdamW [39] for optimization. Following DeiT [54], we use RandAugment [12], Cutmix [70], Mixup [71] and random erasing [74] except the repeated augmentation [28] for data augmentation. For the progressive learning strategy, we set S_e to 224. S_0 is set to 128 for experiments on CIFAR-100 and 160 for experiments on ImageNet. The patch size p is set to 16 following [14]. For the architecture sampler, we use the same batch size and optimization method as the supernet. We initialize the learning rate to 2.5×10^{-4} and 1×10^{-3} for the experiments on CIFAR-100 and ImageNet, respectively. We set the dimension of the hidden state for the LSTM network to 64. The number of training iterations K for $\pi(\cdot; \theta)$ and the hyper-parameter β in Eq. (7) are set to 100 and 0.07, respectively. We set τ to 30 and 40 for the experiments on CIFAR-100 and ImageNet, respectively. For the architecture search stage, we randomly sample 30 architectures and select the architecture with the highest validation accuracy. All the searched architectures directly inherit weights from the learned supernet without any fine-tuning.

4.1 Main Results

We apply our FocusFormer to search ViT architectures under different FLOPs on ImageNet. We show the results in Table 1. For fair comparisons, we modify AutoFormer to use conditional positional encodings [11]. From the results, our searched ViTs perform better than the CNN counterparts, such as ResNet [27], RegNetY [45] and ResNeXt [63], which shows the strong representational power of ViTs. We can also observe that our proposed FocusFormer achieves much higher performance

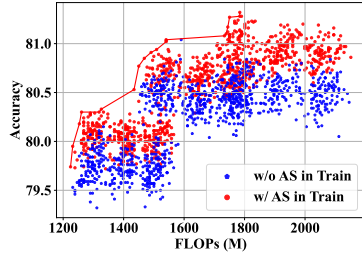


Figure 3: Top-1 accuracy of 1k sub-networks extracted from the supernet-tiny obtained with different training methods on CIFAR-100.

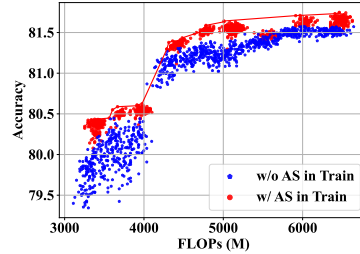


Figure 4: Top-1 accuracy of 1k sub-networks extracted from the supernet-small obtained with different training methods on ImageNet.

Table 2: Effect of the architecture sampler. “AS in Train” denotes that we use architecture sampler rather than uniform sampling [65] to obtain sub-networks during supernet training. “AS in Search” indicates that we use architecture sampler instead of evolutionary search [65] to obtain candidate architectures during search. We report the results of FocusFormer-Ti obtained by different methods on CIFAR-100. “†” denotes that we include the training cost of the architecture sampler.

AS in Train	AS in Search	Top-1 Acc. (%)	FLOPs (G)	Train Cost (GPU Hours)	Search Cost (GPU Hours)
		80.5	1.8	7.7	1.7
✓		81.0	1.8	9.1	1.7
	✓	80.7	1.7	7.7	0.3†
✓	✓	81.0	1.7	9.1	< 0.1

Table 3: Effect of the progressive learning. “PL” represents that we use the progressive learning strategy [53] during supernet training. We report the results of FocusFormer-Ti obtained by different methods on CIFAR-100.

Method	Top-1 Acc. (%)	Top-5 Acc. (%)	FLOPs (G)	Train Cost (GPU Hours)
FocusFormer-Ti w/o PL	80.6	95.8	1.7	11.6
FocusFormer-Ti w/ PL	81.0	96.0	1.7	9.1

than the manually designed ViTs. For example, FocusFormer-Ti with 1.4G FLOPs outperforms DeiT-Ti [54] by 2.9% on the Top-1 accuracy. More critically, our FocusFormer consistently outperforms Autoformer [65] under different resource constraints. For example, with 1.4G FLOPs, FocusFormer-Ti achieves 75.1% in terms of the Top-1 accuracy, which is 0.5% higher than AutoFormer-Ti.

4.2 Further Studies

Effect of the architecture sampler. To investigate the effect of our architecture sampler (“AS”), we apply “AS” to different stages. Specifically, applying the “AS” in the supernet training stage denotes that we sample sub-networks from the learned distribution using “AS” instead of a uniform distribution [65] while applying the “AS” in the search stage represents that we obtain candidate architectures using “AS” rather than the evolutionary methods [65]. The results are provided in Table 2. To show the supernet performance under various resource constraints, we also randomly sample 1k architectures from the supernet and show the results in Figures 3 and 4.

From the results, using the “AS” in the supernet training stage introduces a little training cost but consistently improves the performance under various resource constraints (See Figures 3 and 4). The performance improvement is more significant in high FLOPs scenarios. For example, with about 1.7G FLOPs, our method with “AS” in the supernet training stage outperforms those without “AS” by 0.5% in terms of the Top-1 accuracy on CIFAR-100. Moreover, using our “AS” in the search stage achieves comparable or even better performance than the evolutionary search while significantly reducing the search cost (0.3 vs. 1.7 GPU Hours). Using “AS” in both the training stage and search stage, our FocusFormer yields the best performance with 81.0% Top-1 accuracy and 1.7G FLOPs while the search cost is less than 0.1 GPU Hour. These results show that our “AS” is able to improve the performance of the searched architectures while significantly reducing the search cost.

Table 4: Performance comparisons with different update intervals τ on CIFAR-100.

Model	τ	Top-1 Acc. (%)	Top-5 Acc. (%)	#Params (M)	FLOPs (G)
FocusFormer-Ti	10	80.3	95.9	8.1	1.8
	20	81.0	96.0	8.0	1.7
	30	80.8	96.1	7.8	1.7
	40	80.5	95.9	8.0	1.8

Table 5: Performance comparisons with different step sizes s on CIFAR-100.

Model	s	Top-1 Acc. (%)	Top-5 Acc. (%)	#Params (M)	FLOPs (G)
FocusFormer-Ti	50	80.4	96.0	7.7	1.7
	100	80.4	95.8	7.9	1.7
	200	81.0	96.0	8.0	1.7
	300	80.5	95.8	7.9	1.7
	400	80.8	95.9	7.9	1.7
	500	80.3	95.7	7.7	1.7

Effect of the progressive learning. To investigate the effect of progressive learning (See Section 3.2), we apply our method to obtain architectures with and without progressive learning during supernet training. From Table 3, FocusFormer with “PL” strategy improves the supernet performance by 0.4% on the Top-1 accuracy while significantly reducing the training cost by 2.5 GPU Hours. Therefore, we use progressive learning by default.

Effect of different update intervals τ . To investigate the effect of different update intervals τ in the supernet training stage, we train FocusFormer-Ti with different $\tau \in \{10, 20, 30, 40\}$ and show the results in Table 4. From the results, with the decrease of τ , the performance of the searched architecture becomes better first and then goes worse. For example, the searched architecture obtained by $\tau = 30$ with 0.1G lower FLOPs surpasses that of $\tau = 40$ by 0.3% in terms of the Top-1 accuracy. One possible reason is that we need to update the architecture sampler regularly to a certain extent to accommodate the performance change during supernet training. However, too small τ indicates the frequent changes of the learned architectural distribution. As a result, the potentially good architectures may not be sufficiently trained. Moreover, as our FocusFormer achieves the best performance when τ is set to 20, we use it by default in our experiments.

Effect of different step sizes s . To investigate the effect of different step sizes s in resource constraint discretization, we train FocusFormer-Ti with different $s \in \{50, 100, 200, 300, 400, 500\}$. Here, smaller s denotes more resource constraint candidates. From Table 5, the performance of searched architecture becomes better and then worsens with the decrease of s . On one hand, larger s results in a small number of resource constraint candidates, which can not accurately represent an arbitrary resource constraint due to coarse-grained linear interpolation. For example, our method yields the worst performance with $s = 500$.

On the other hand, smaller s leads to a large number of resource constraint candidates, which introduces too many learnable embedding vectors and hence incurs the optimization difficulty. With $s = 200$, the searched architectures achieve the best performance (81.0% in terms of the Top-1 accuracy).

5 Conclusion and Future Work

In this paper, we have proposed FocusFormer to mitigate the gap between training and deployment in one-shot neural architecture search. To this end, we have devised an architecture sampler to obtain ViT architectures that are likely on the Pareto frontier under diverse resource constraints. By jointly training the architecture sampler with network parameters, we put more training resources on these salient architectures and hence improve the performance of the searched ViT architectures. Once the supernet and architecture sampler have been well-trained, we can directly use our proposed architecture sampler to obtain architectures with promising performance while satisfying the given resource constraint. Experiments on CIFAR-100 and ImageNet have demonstrated that our proposed method is able to improve the performance of the searched architectures while significantly reducing the search cost. In the future, we may extend our method in several aspects. First, we may consider improving both the training and search efficiency by using some sparsity training strategies. Second,

we may jointly perform neural architecture search and quantization simultaneously to obtain more compact ViTs with comparable performance.

References

- [1] J. L. Ba, J. R. Kiros, and G. E. Hinton. Layer normalization. *arXiv preprint arXiv:1607.06450*, 2016.
- [2] G. Bender, P.-J. Kindermans, B. Zoph, V. Vasudevan, and Q. Le. Understanding and simplifying one-shot architecture search. In *ICML*, pages 550–559, 2018.
- [3] G. Bender, H. Liu, B. Chen, G. Chu, S. Cheng, P.-J. Kindermans, and Q. V. Le. Can weight sharing outperform random architecture search? an investigation with tunas. In *CVPR*, pages 14323–14332, 2020.
- [4] H. Cai, C. Gan, T. Wang, Z. Zhang, and S. Han. Once-for-all: Train one network and specialize it for efficient deployment. In *ICLR*, 2020.
- [5] H. Cai, L. Zhu, and S. Han. ProxylessNAS: Direct neural architecture search on target task and hardware. In *ICLR*, 2019.
- [6] N. Carion, F. Massa, G. Synnaeve, N. Usunier, A. Kirillov, and S. Zagoruyko. End-to-end object detection with transformers. In *ECCV*, pages 213–229, 2020.
- [7] M. Chen, K. Wu, B. Ni, H. Peng, B. Liu, J. Fu, H. Chao, and H. Ling. Searching the search space of vision transformer. *NeurIPS*, 34, 2021.
- [8] X. Chen, H. Wang, and B. Ni. X-volution: on the unification of convolution and self-attention. *arXiv preprint arXiv:2106.02253*, 2021.
- [9] B. Cheng, A. Schwing, and A. Kirillov. Per-pixel classification is not all you need for semantic segmentation. *NeurIPS*, 34, 2021.
- [10] X. Chu, Z. Tian, Y. Wang, B. Zhang, H. Ren, X. Wei, H. Xia, and C. Shen. Twins: Revisiting the design of spatial attention in vision transformers. *NeurIPS*, 34, 2021.
- [11] X. Chu, Z. Tian, B. Zhang, X. Wang, X. Wei, H. Xia, and C. Shen. Conditional positional encodings for vision transformers. *arXiv preprint arXiv:2102.10882*, 2021.
- [12] E. D. Cubuk, B. Zoph, J. Shlens, and Q. Le. Randaugment: Practical automated data augmentation with a reduced search space. In *NeurIPS*, 2020.
- [13] J. Deng, W. Dong, R. Socher, L.-J. Li, K. Li, and L. Fei-Fei. Imagenet: A large-scale hierarchical image database. In *CVPR*, pages 248–255, 2009.
- [14] A. Dosovitskiy, L. Beyer, A. Kolesnikov, D. Weissenborn, X. Zhai, T. Unterthiner, M. Dehghani, M. Minderoeder, G. Heigold, S. Gelly, J. Uszkoreit, and N. Houlsby. An image is worth 16x16 words: Transformers for image recognition at scale. In *ICLR*, 2021.
- [15] S. d’Ascoli, H. Touvron, M. L. Leavitt, A. S. Morcos, G. Biroli, and L. Sagun. Convit: Improving vision transformers with soft convolutional inductive biases. In *ICML*, pages 2286–2296, 2021.
- [16] A. Fan, E. Grave, and A. Joulin. Reducing transformer depth on demand with structured dropout. In *ICLR*, 2020.
- [17] H. Fan, B. Xiong, K. Mangalam, Y. Li, Z. Yan, J. Malik, and C. Feichtenhofer. Multiscale vision transformers. In *ICCV*, pages 6824–6835, 2021.
- [18] C. Gong, D. Wang, M. Li, X. Chen, Z. Yan, Y. Tian, qiang liu, and V. Chandra. NASvit: Neural architecture search for efficient vision transformers with gradient conflict aware supernet training. In *ICLR*, 2022.
- [19] B. Graham, A. El-Nouby, H. Touvron, P. Stock, A. Joulin, H. Jégou, and M. Douze. Levit: a vision transformer in convnet’s clothing for faster inference. In *ICCV*, pages 12259–12269, 2021.
- [20] J. Guo, K. Han, H. Wu, C. Xu, Y. Tang, C. Xu, and Y. Wang. Cmt: Convolutional neural networks meet vision transformers. *arXiv preprint arXiv:2107.06263*, 2021.
- [21] Y. Guo, Y. Chen, Y. Zheng, Q. Chen, P. Zhao, J. Chen, J. Huang, and M. Tan. Pareto-frontier-aware neural architecture generation for diverse budgets. *arXiv preprint arXiv:2103.00219*, 2021.
- [22] Y. Guo, Y. Chen, Y. Zheng, P. Zhao, J. Chen, J. Huang, and M. Tan. Breaking the curse of space explosion: Towards efficient nas with curriculum search. In *ICML*, pages 3822–3831, 2020.
- [23] Z. Guo, X. Zhang, H. Mu, W. Heng, Z. Liu, Y. Wei, and J. Sun. Single path one-shot neural architecture search with uniform sampling. In *ECCV*, pages 544–560. Springer, 2020.
- [24] K. Han, A. Xiao, E. Wu, J. Guo, C. Xu, and Y. Wang. Transformer in transformer. *NeurIPS*, 34, 2021.
- [25] C. He, H. Ye, L. Shen, and T. Zhang. Milenas: Efficient neural architecture search via mixed-level reformulation. In *CVPR*, pages 11993–12002, 2020.

- [26] H. He, J. Liu, Z. Pan, J. Cai, J. Zhang, D. Tao, and B. Zhuang. Pruning self-attentions into convolutional layers in single path. *arXiv preprint arXiv:2111.11802*, 2021.
- [27] K. He, X. Zhang, S. Ren, and J. Sun. Deep residual learning for image recognition. In *CVPR*, pages 770–778, 2016.
- [28] E. Hoffer, T. Ben-Nun, I. Hubara, N. Giladi, T. Hoefler, and D. Soudry. Augment your batch: better training with larger batches. *arXiv preprint arXiv:1901.09335*, 2019.
- [29] A. Howard, M. Sandler, G. Chu, L.-C. Chen, B. Chen, M. Tan, W. Wang, Y. Zhu, R. Pang, V. Vasudevan, et al. Searching for mobilenetv3. In *ICCV*, pages 1314–1324, 2019.
- [30] S.-Y. Huang and W.-T. Chu. Searching by generating: Flexible and efficient one-shot nas with architecture generator. In *CVPR*, pages 983–992, 2021.
- [31] T. Huang, S. You, F. Wang, C. Qian, C. Zhang, X. Wang, and C. Xu. Greedynasv2: Greedier search with a greedy path filter. *arXiv preprint arXiv:2111.12609*, 2021.
- [32] A. Krizhevsky and G. Hinton. Learning multiple layers of features from tiny images. Technical Report 0, University of Toronto, Toronto, Ontario, 2009.
- [33] C. Li, B. Zhuang, G. Wang, X. Liang, X. Chang, and Y. Yang. Automated progressive learning for efficient training of vision transformers. In *CVPR*, 2022.
- [34] L. Li and A. Talwalkar. Random search and reproducibility for neural architecture search. In *UAI*, pages 367–377, 2020.
- [35] Y. Li, K. Zhang, J. Cao, R. Timofte, and L. Van Gool. Localvit: Bringing locality to vision transformers. *arXiv preprint arXiv:2104.05707*, 2021.
- [36] H. Liu, K. Simonyan, and Y. Yang. DARTS: differentiable architecture search. In *ICLR*, 2019.
- [37] Z. Liu, Y. Lin, Y. Cao, H. Hu, Y. Wei, Z. Zhang, S. Lin, and B. Guo. Swin transformer: Hierarchical vision transformer using shifted windows. In *ICCV*, pages 10012–10022, 2021.
- [38] I. Loshchilov and F. Hutter. SGDR: stochastic gradient descent with warm restarts. In *ICLR*, pages 1–16, 2017.
- [39] I. Loshchilov and F. Hutter. Decoupled weight decay regularization. In *ICLR*, 2019.
- [40] Z. Lu, K. Deb, E. Goodman, W. Banzhaf, and V. N. Boddeti. Nsganetv2: Evolutionary multi-objective surrogate-assisted neural architecture search. In *ECCV*, pages 35–51, 2020.
- [41] Z. Lu, I. Whalen, V. Boddeti, Y. Dhebar, K. Deb, E. Goodman, and W. Banzhaf. Nsga-net: neural architecture search using multi-objective genetic algorithm. In *Proceedings of the genetic and evolutionary computation conference*, pages 419–427, 2019.
- [42] Z. Pan, B. Zhuang, J. Liu, H. He, and J. Cai. Scalable vision transformers with hierarchical pooling. In *ICCV*, pages 377–386, 2021.
- [43] H. Pham, M. Guan, B. Zoph, Q. Le, and J. Dean. Efficient neural architecture search via parameters sharing. In *ICML*, pages 4095–4104, 2018.
- [44] A. Radford, L. Metz, and S. Chintala. Unsupervised representation learning with deep convolutional generative adversarial networks. In *ICLR*, 2016.
- [45] I. Radosavovic, R. P. Kosaraju, R. Girshick, K. He, and P. Dollár. Designing network design spaces. In *CVPR*, pages 10428–10436, 2020.
- [46] E. Real, A. Aggarwal, Y. Huang, and Q. V. Le. Regularized evolution for image classifier architecture search. In *AAAI*, pages 4780–4789, 2019.
- [47] E. Real, S. Moore, A. Selle, S. Saxena, Y. L. Suematsu, J. Tan, Q. V. Le, and A. Kurakin. Large-scale evolution of image classifiers. In *ICML*, pages 2902–2911, 2017.
- [48] R. Ru, P. Esperanca, and F. M. Carlucci. Neural architecture generator optimization. *NeurIPS*, 33:12057–12069, 2020.
- [49] M. Sandler, A. Howard, M. Zhu, A. Zhmoginov, and L.-C. Chen. Mobilenetv2: Inverted residuals and linear bottlenecks. In *CVPR*, pages 4510–4520, 2018.
- [50] D. So, Q. Le, and C. Liang. The evolved transformer. In *ICML*, pages 5877–5886, 2019.
- [51] A. Srinivas, T.-Y. Lin, N. Parmar, J. Shlens, P. Abbeel, and A. Vaswani. Bottleneck transformers for visual recognition. In *CVPR*, pages 16519–16529, 2021.
- [52] M. Tan, B. Chen, R. Pang, V. Vasudevan, M. Sandler, A. Howard, and Q. V. Le. Mnasnet: Platform-aware neural architecture search for mobile. In *CVPR*, pages 2820–2828, 2019.
- [53] M. Tan and Q. Le. Efficientnetv2: Smaller models and faster training. In *ICML*, pages 10096–10106, 2021.

- [54] H. Touvron, M. Cord, M. Douze, F. Massa, A. Sablayrolles, and H. Jégou. Training data-efficient image transformers & distillation through attention. In *ICML*, pages 10347–10357, 2021.
- [55] A. Vaswani, N. Shazeer, N. Parmar, J. Uszkoreit, L. Jones, A. N. Gomez, Ł. Kaiser, and I. Polosukhin. Attention is all you need. *NeurIPS*, 30, 2017.
- [56] D. Wang, M. Li, C. Gong, and V. Chandra. Attentivenas: Improving neural architecture search via attentive sampling. In *CVPR*, pages 6418–6427, 2021.
- [57] H. Wang, Z. Wu, Z. Liu, H. Cai, L. Zhu, C. Gan, and S. Han. HAT: hardware-aware transformers for efficient natural language processing. In D. Jurafsky, J. Chai, N. Schluter, and J. R. Tetreault, editors, *ACL*, pages 7675–7688, 2020.
- [58] W. Wang, E. Xie, X. Li, D.-P. Fan, K. Song, D. Liang, T. Lu, P. Luo, and L. Shao. Pyramid vision transformer: A versatile backbone for dense prediction without convolutions. In *ICCV*, pages 568–578, 2021.
- [59] R. J. Williams. Simple statistical gradient-following algorithms for connectionist reinforcement learning. *Machine learning*, 8(3):229–256, 1992.
- [60] B. Wu, X. Dai, P. Zhang, Y. Wang, F. Sun, Y. Wu, Y. Tian, P. Vajda, Y. Jia, and K. Keutzer. Fbnet: Hardware-aware efficient convnet design via differentiable neural architecture search. In *CVPR*, pages 10734–10742, 2019.
- [61] H. Wu, B. Xiao, N. Codella, M. Liu, X. Dai, L. Yuan, and L. Zhang. Cvt: Introducing convolutions to vision transformers. In *ICCV*, pages 22–31, 2021.
- [62] K. Wu, H. Peng, M. Chen, J. Fu, and H. Chao. Rethinking and improving relative position encoding for vision transformer. In *ICCV*, pages 10033–10041, 2021.
- [63] S. Xie, R. Girshick, P. Dollár, Z. Tu, and K. He. Aggregated residual transformations for deep neural networks. In *CVPR*, pages 1492–1500, 2017.
- [64] S. Xie, A. Kirillov, R. Girshick, and K. He. Exploring randomly wired neural networks for image recognition. In *ICCV*, pages 1284–1293, 2019.
- [65] J. Xu, J. Wang, M. Long, et al. Autoformer: Decomposition transformers with auto-correlation for long-term series forecasting. *NeurIPS*, 34, 2021.
- [66] Y. Xu, Q. Zhang, J. Zhang, and D. Tao. Vitae: Vision transformer advanced by exploring intrinsic inductive bias. *NeurIPS*, 34, 2021.
- [67] S. You, T. Huang, M. Yang, F. Wang, C. Qian, and C. Zhang. Greedynas: Towards fast one-shot nas with greedy supernet. In *CVPR*, pages 1999–2008, 2020.
- [68] J. Yu, P. Jin, H. Liu, G. Bender, P.-J. Kindermans, M. Tan, T. Huang, X. Song, R. Pang, and Q. Le. Bignas: Scaling up neural architecture search with big single-stage models. In *ECCV*, pages 702–717, 2020.
- [69] L. Yuan, Y. Chen, T. Wang, W. Yu, Y. Shi, Z.-H. Jiang, F. E. Tay, J. Feng, and S. Yan. Tokens-to-token vit: Training vision transformers from scratch on imagenet. In *ICCV*, pages 558–567, 2021.
- [70] S. Yun, D. Han, S. J. Oh, S. Chun, J. Choe, and Y. Yoo. Cutmix: Regularization strategy to train strong classifiers with localizable features. In *ICCV*, pages 6023–6032, 2019.
- [71] H. Zhang, M. Cisse, Y. N. Dauphin, and D. Lopez-Paz. mixup: Beyond empirical risk minimization. In *ICLR*, 2018.
- [72] Y. Zhao, L. Dong, Y. Shen, Z. Zhang, F. Wei, and W. Chen. Memory-efficient differentiable transformer architecture search. In *ACL*, pages 4254–4264, 2021.
- [73] S. Zheng, J. Lu, H. Zhao, X. Zhu, Z. Luo, Y. Wang, Y. Fu, J. Feng, T. Xiang, P. H. Torr, et al. Rethinking semantic segmentation from a sequence-to-sequence perspective with transformers. In *CVPR*, pages 6881–6890, 2021.
- [74] Z. Zhong, L. Zheng, G. Kang, S. Li, and Y. Yang. Random erasing data augmentation. In *AAAI*, pages 13001–13008, 2020.
- [75] B. Zoph and Q. V. Le. Neural architecture search with reinforcement learning. In *ICLR*, 2017.

Supplementary Material for FocusFormer: Focusing on What We Need via Architecture Sampler

A Visualization of the searched architectures

In this section, we show the ViT architectures obtained by our FocusFormer in Figure A. The searched architectures tend to select large Q-K-V dimensions, MLP ratios, head numbers, and depth numbers with the increase of FLOPs and #Params. For FocusFormer-S and FocusFormer-B, we observe that the intermediate Transformer blocks prefer large head numbers, while the deep blocks tend to choose small head numbers.

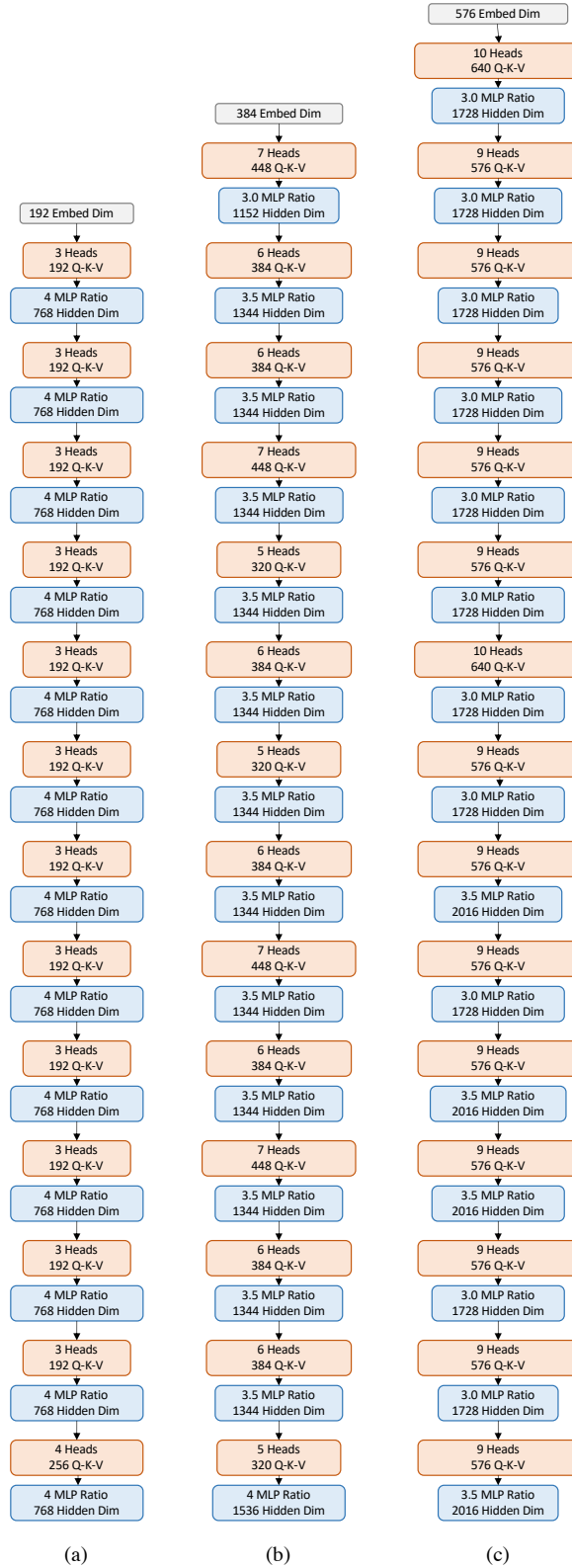


Figure A: The architectures obtained by FocusFormer under different resource constraints on ImageNet. The orange and blue blocks denote the multi-head self-attention layers and MLP blocks, respectively. We omit the shortcuts and conditional positional encodings for simplicity. (a): The searched architecture of FocusFormer-Ti with 1.4G FLOPs and 6.2M #Params. (b): The searched architecture of FocusFormer-S with 5.0G FLOPs and 23.7M #Params. (c): The searched architecture of FocusFormer-B with 11.0G FLOPs and 52.7M #Params.